v. 2, n. 5, 2022

Journal of
Engineering
Research

STUDY OF THE IMPACT OF TEMPERATING SIMULTANEOUS TO THE BENDING PROCESS OF ALUMINUM ALLOY ABNT 6061

Guilherme Oliveira Goulart
Master Student, Universidade do Vale do Rio dos Sinos, Brazil

Lauro Côrrea Romeiro
Prof. Dr, institution: Universidade Federal do Rio Grande do Sul, Brazil

All content in this magazine is licensed under a Creative Commons Attribution License. Attribution-Non-Commercial-Non-Derivatives 4.0 International (CC BY-NC-ND 4.0).

Abstract: The weight reduction of components, without affecting the mechanical strength, has become one of the focuses of the naval, aeronautical and automotive industries, and aluminum alloys have these characteristics when compared to many forged steel components, making it possible to obtain high mechanical strength associated with them. to its low density. This study presents the development of a simultaneous hot forming and quenching process for aluminum alloy 6061. The development of the process began with numerical simulation rounds seeking to establish an optimized geometry for the tool. Numerical simulations of heat exchange, hot and cold forming and tool stresses were performed. The samples were heated in an electric heating oven, manually placed in the die, and shaped in an MTS Landmark testing machine, used as a press, with the lower die serving as a container for the fluid, which comes into contact with the body of proof during forming. The aim of this study was to eliminate heating operations to solubilize the alloy, usually necessary in industrial processes, aiming to achieve formability and hardness after the aging heat treatment, and also seeking greater productivity and energy performance in the industrial environment. For comparison, tests were also carried out with samples following the traditional process, samples with quenching after forming and cold-formed samples. The results obtained by the study were promising in relation to the development of the process, as it presented a dimensional closer to the determined measures, and also resulted in parts with excellent finishing.
Keywords: Alloy 6061, Conformation, Simultaneity, Quenching, Solubilization.

INTRODUCTION

Large plastic deformations without defects are possible in hot forging as long as the stress flux is reduced and work hardening does not occur at high temperatures [3]. Within the field of study of forming processes, the bending process is simple and has a low manufacturing cost, and can be applied in components from simple geometry to complex structures [4].

The work consisted in the study of alloy 6061 being folded and precipitated through different forms, aiming to analyze the impact of these variations, starting with the conventional process of forming, heating and tempering, according to a parametric process taking advantage of the residual temperature of the forming to carry out tempering, sequentially the objective process of this article performing the quenching simultaneously with the forming and finally a cold forming process for load analysis.

BIBLIOGRAPHIC REVIEW

ALUMINUM ALLOY 6061

The designated alloys of the 6XXX series are heat treatable alloys and considered of medium strength, as a characteristic, they have excellent deformability and corrosion resistance, characteristics obtained through the main alloying elements, magnesium (Mg) and silicon (Si), responsible for increasing the hardness of 6XXX alloys through precipitation hardening [2].

V-FOLDING

Process that uses press brakes, responsible for providing energy and necessary movements, apply a force performing deformation by bending the part, resulting in a linear bend, with the angle of the part varying according to the profile of the set of dies. There are several forms of folding presented in several literatures [4].

QUENCHING AND SOLUBILIZATION

The basic principle of hardening an alloy is to reduce the solubilization limit as the temperature decreases. The alloy must be heated to high temperatures, varying from alloy to alloy, and subsequently cooled by immersion in fluid, performing quenching. Rapid cooling suppresses theta phase separation, causing the alloy to exist at an unstable low temperature in a supersaturated state. If after quenching the alloy is aged long enough, the secondary phase will be precipitated [1].

The presence of the precipitated beta phase allows significant changes in the mechanical behavior of the material. Mainly in the yield strength and hardness, which are improved and present a linear relationship [2].

MATERIALS AND METHODS

The equipment was chosen according to the availability of the Mechanical Testing, Physical Metallurgy, Foundry and ITT Fuse laboratories at the Universidade do Vale do Rio dos Sinos – UNISINOS. Figure 1 presents the flowchart of the methodology used in this study.

EQUIPMENT USED AT WORK

To carry out the study, the existing resources in the UNISINOS laboratories were used for machining the dies, heating, forming, instrumenting and measuring the specimens. Software were also used for CAD modeling and numerical simulation of conformations and temperature change.

- Rocco milling machine model RFV-1-A;
- 3-axis CNC milling machine ROMI model Polaris V400;
- Universal Landmark MTS Testing Machine: 25 tf (245.2 kN);
- SANCHIS oven (UNISINOS' own assembly);
- 2.6 kW SANCHIS Att oven;
- Forno De Leo & Cia Ltda, 4 A;
- LT Lutron TM-909 pyrometer;
- Mitutoyo HR-400 durometer with Brinell kit;
- Starret Profile Projector model HE-400;
- Siemens NX version 12 CAD "Software";
- Siemens NX "Software" version 1899 CAM;
- "Software" QForm Numerical Simulation version VX8.2.3.

BODY OF TEST

The definitions of the specimens were established according to the following limiting parameters by the resources used: Inductor diameter, press capacity and tool dimension.

Due to the fact that the inductors of the oven used have a gauge of Ø68 mm, a maximum width of 40 mm was established for the specimen, aiming at a gap between the inductor and the specimen.

To carry out the forming, the press used has a nominal capacity of 25 tf (245.2 kN) with a useful pressing force, according to safety regulations, of 19 tf (186.3 kN).

The thickness was defined at 13.0 mm, as this is the minimum supply measure for aluminum sheets for heat treatment, according to supplier availability. Numerical simulations of the process were performed, ensuring that such thickness does not exceed the limit of the press used for forming.

MATRIX

The geometry of the matrix was defined from the geometry of the specimen and based on the dimensions of the specimen with the idealized deformation for the study.

This way, simulations were carried out to validate the machinability through the CAM, aiming to avoid very deep cavities so as not to break the tools as well as the resistance of the tool for the conformation of the twenty-eight specimens.

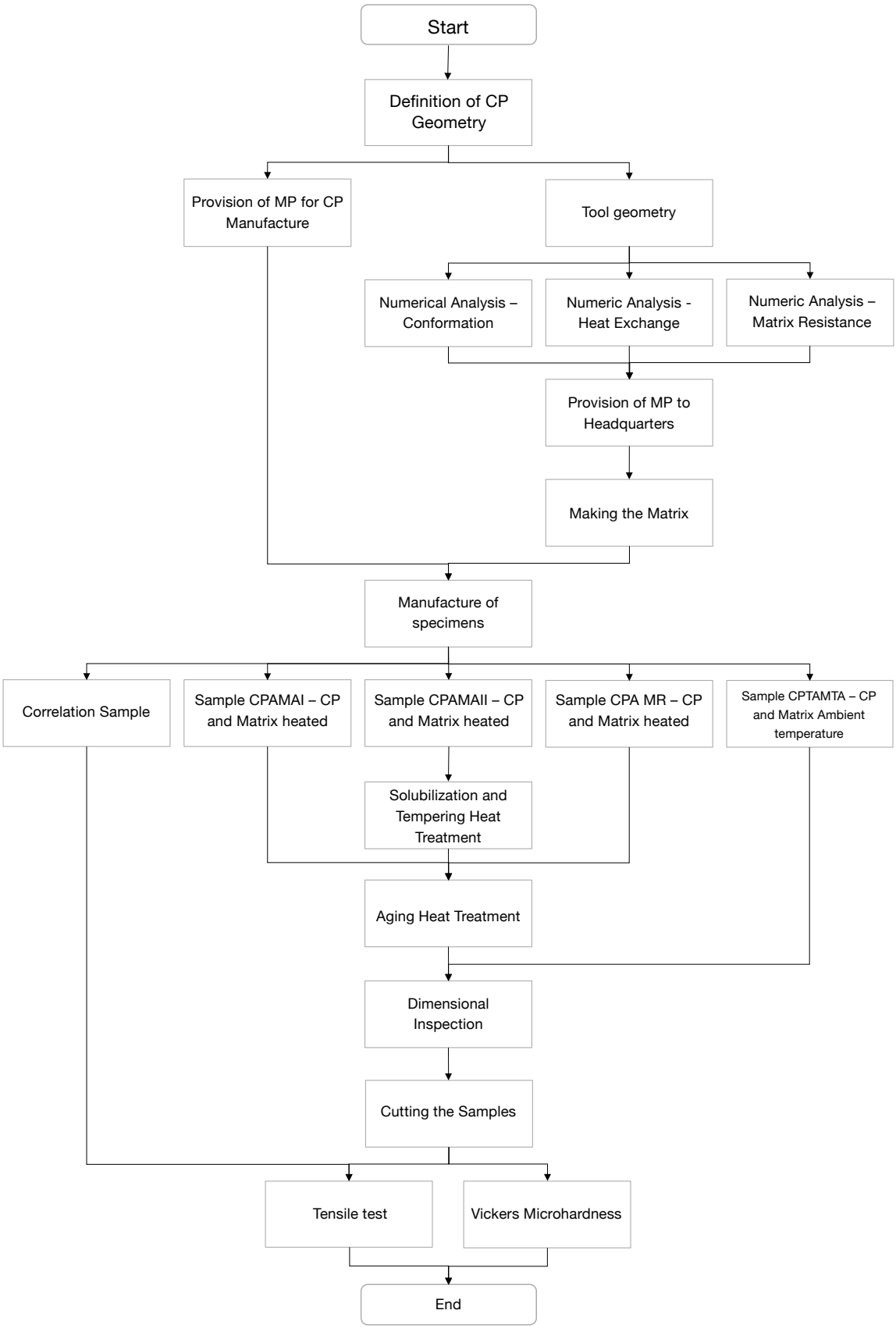

Figure 1 - Flowchart Methodology.

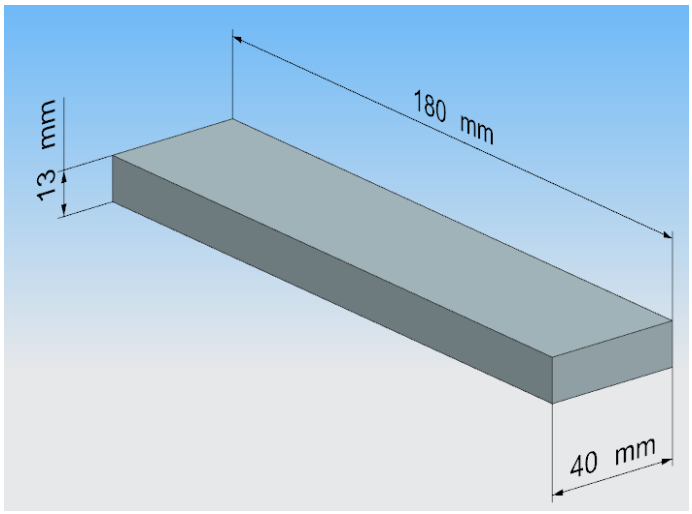

Figure 2 - Specimen.

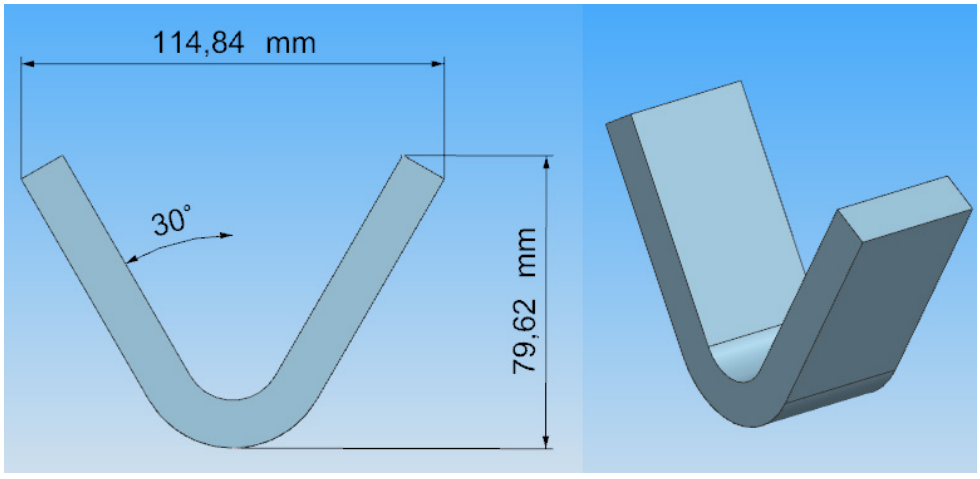

Figure 3 - Specimen After Deformation.

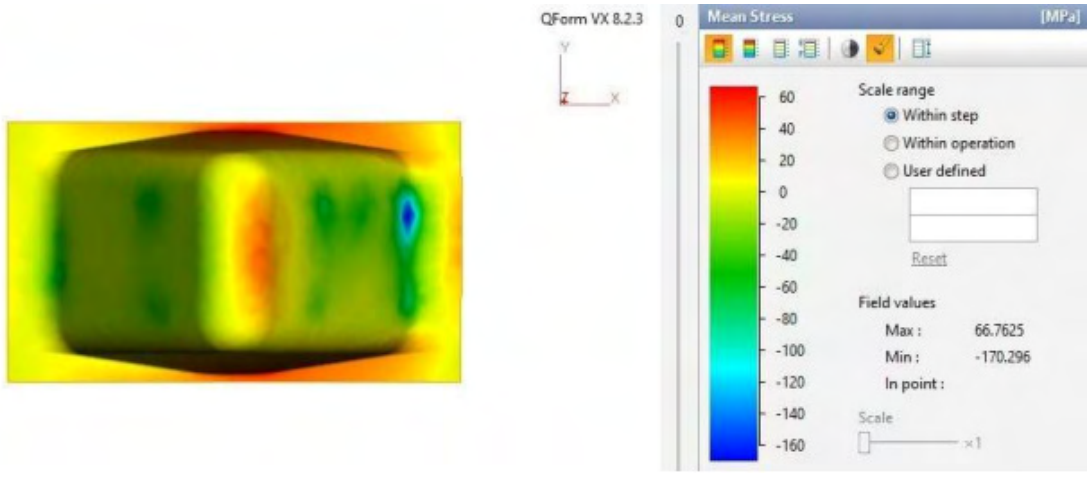

Figure 4 - Main Stresses in the Lower Matrix.

Simulations of the bending process were carried out, in addition to the definition of the process pressing forces, also for analysis of the stresses in the tool, with this it was determined that the lower tool suffers the most severe requests of the process, being then used as a basis to determine the matrix life.

With the results of the main stresses, the calculation began to determine the useful life of the tool, considering the material of carbon steel 1045 for the dies. By calculating the number of cycles [6] an estimated useful life of approximately 2.95x105 was reached, that is, the matrix with the established geometry and in 1045 supports the amount of samples to be produced.

From the CAD project and the validation of the material and useful life of the die, two blocks of 1045 steel were acquired and then the post processing was generated via CAM for machining the dies.

FOLDING PROCESS

As it was shown in the methodology flowchart, the specimens were separated into 4 families, containing 7 bars in each, where each family underwent a different processing.

Table 2 shows the temperatures for the forming process.

SOLUBILIZATION PROCESS

The solubilization heat treatment was carried out only in the CPAMA I family, since solubilization was not carried out in the CPTAMTA family, solubilization carried out during conformation in the CPAMR process and solubilization carried out after conformation in the CPAMA II family. This way, the samples of the CPAMA I family were heated to a temperature of 530°C for one hour, later they were immersed in water at room temperature, approximately 20°C. The samples were heated in a 220 V, 2.6 kW Sanchis Att model oven, in the Physical Metallurgy laboratory of the Universidade do Vale do Rio dos Sinos – Unisinos. The temperature was measured with a pyrometer located close to the pieces.

AGING PROCESS

The CPAMA I, CPAMA II and CPAMR family samples were heated in an oven to a temperature of 180°C for 18 hours and cooled in air for aging treatment. The samples were heated in a De Leo et al. Ltd, 4 A and 220 V, from the Foundry Laboratory of the University of Vale do Rio dos Sinos – Unisinos. The temperature measurement was performed with a thermometer positioned close to the pieces.

Heating was carried out in two batches, the first with 4 specimens from each family and the second with the remaining specimens, in order to avoid the loss of specimens in case any unforeseen event occurred during the 18 hours of heating.

TESTS AND INSPECTIONS

After all processing, the results were evaluated by visual inspection in the central region of the specimen, to analyze the presence of cracks. Dimensional inspection in the dimensions shown in figure 7.

Subsequently, 6 points were analyzed on the specimen cover for hardness validation. Finally, an inspection by SEM and EDS of 4 specimens, one from each family, was carried out in the central region, the main deformed region.

EXPERIMENTAL ANALYSIS

This topic contains the results obtained from the processes as well as the results obtained from the analyses, and at the end of each subtopic, contains the discussions of the results found.

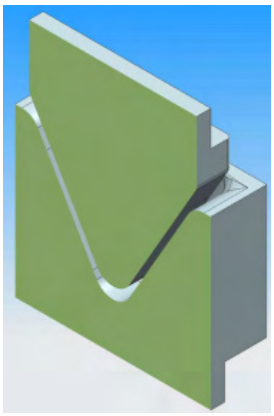

Figure 5 - Isometric View of the Matrix.

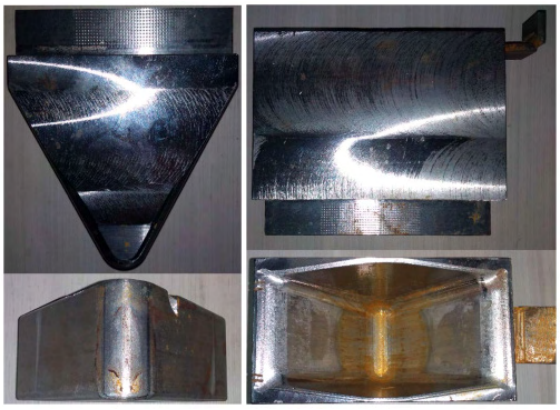

Figure 6 - Machined Upper and Lower Die.

Family	Body of Test	Matrix	Conformation	Solubilization	Aging
CPAMA I	Warme	Warmed	Hot	After cooling the CP	Yes
CPAMA II	Warmed	Warmed	Hot	Sequential to conformation	Yes
CPAMR	Warmed	Cooled	Simultaneous	During forming	Yes
CPTAMTA	Room temperature	Room temperature	Cold	No	No

Table 1 - Process Detailing.

Family	Temperature - Piece	Temperature - Matrix
CPAMA I	530°C	70°C
CPAMA II	530°C	70°C
CPAMR	530°C	20°C
CPTAMTA	Ambiente	Ambiente

Tabela 2 - Temperaturas para Conformação.

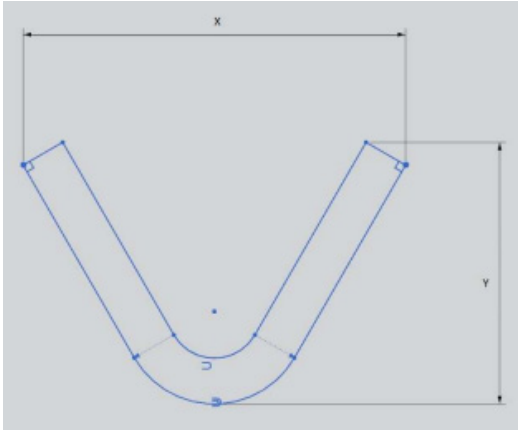

Figure 7 - Dimensional Inspection.

FOLDING

In this topic, the bending pressing forces of each family will be shown, as detailed in topic 3.4 of this article. So that figure 8 presents the results obtained for the CPAMR samples, figure 9 the results obtained for the CPAMA I samples, figure 10 the results obtained for the CPAMA II samples and finally, figure 11 presents the results obtained for the CPTAMTA samples.

- CPAMR:

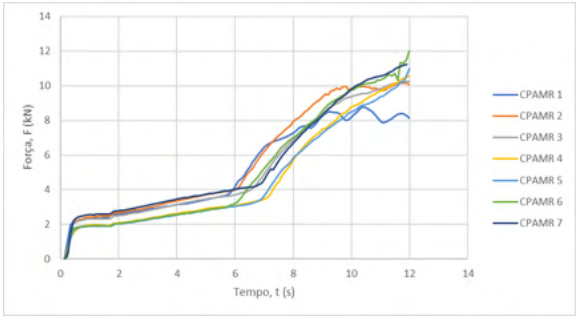

Figure 8 - Press Force x CPAMR Time Graph

- CPAMA I:

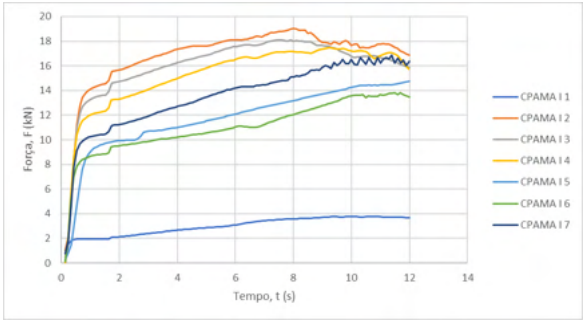

Figure 9 - Pressing Force x Time CPAMA I graph

- CPAMA II:

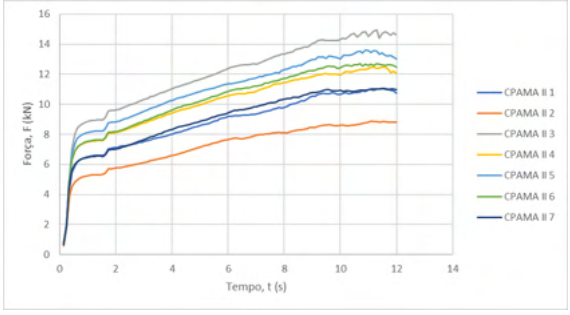

Figure 10 - CPAMA II Press Force x Time Chart

- CPTAMTA:

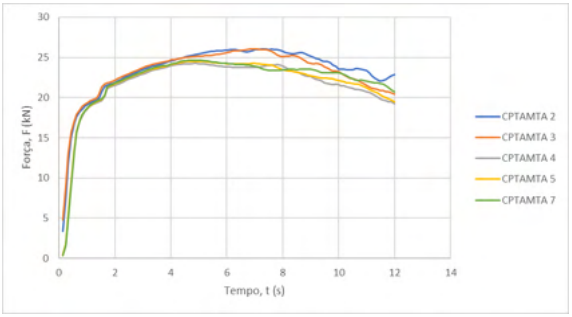

Figure 11 - Pressing Force x Time CPTAMTA Chart

With the results obtained in the conformation, the pressing forces of the specimens that resulted in the highest pressing forces of each family were separated and a graph of the greatest requests of the press, per family, was generated.

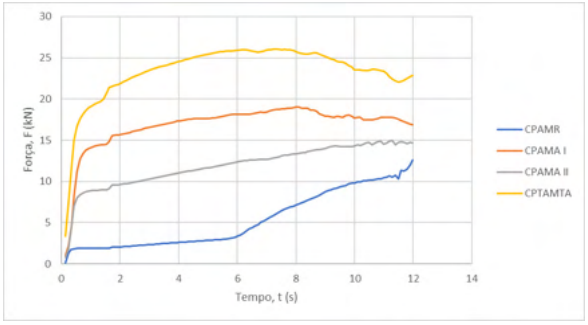

Figure 12 - Graph of Pressing Force x Comparative Time between Families

According to the results shown in Figure 12, it is possible to validate that the cold deformation process, represented by the CPTAMTA sample family, requires greater capacity of the press than the other hot processes.

SOLUBILIZATION AND AGING HEAT TREATMENT

The parameters presented in topics 3.5 and 3.6 were followed, without any changes. The evaluation of the parameters used will be validated in topics 4.5 and 4.6.

VISUAL INSPECTION

The CPTAMTA samples, which underwent cold forming, all showed cracks, and two of them broke during forming. Cracks which are shown in figure 13.

The samples that were hot formed were all approved in the visual inspection, with no incidence of forming cracks or thermal cracks. As shown in figure 14.

With this, it is possible to determine the degree of requirement of cold forming when compared to hot forming, with 100% of the cold formed samples rejected by crack and 28.7% of them broke during forming. It is possible to conclude that the crack comes from cold forming, as they were generated only in the conformation processes of the CPTAMTA family. Another statement that can be made, based on the results obtained in the visual inspection, is that the solubilization and aging processes did not generate thermal cracks in any of the families.

DIMENSIONAL INSPECTION

The dimensional analysis of the samples was performed with a universal analog mitutoyo caliper, following the dimensions established in figure 3 of this article. The results were compiled generating table 3.

Samples CPTAMTA 1 and CPTAMTA 6 suffered breakage during the process, even so they were measured, the values are shown in the table to relate approximately to the dimension when the sample broke. Another observation regarding the dimensional inspection is that due to the inaccuracy in the measurement of the "Y" dimension, they are shown in the table only as a reference.

Applying the mean and standard deviation to the results found, it was possible to generate table 4.

With the values shown in table 4, the samples that came closest to the planned dimension, in X, were the CPAMR samples, in addition to being the process with the least variation between the samples, due to the smaller resulting standard deviation, both before and after the aging heat treatment. It is also possible to observe that the deviation remained the same before and after the heat treatment for the CPAMR samples, noting that for the other samples that underwent heat treatment, there was a change in the value of their deviations.

HARDNESS TEST

The first step in carrying out the hardness tests on the specimens was the definition of the measurement points.

As the specimens were symmetrical, hardness measurements were taken on only one side, with three measurements on the inside of the specimen and three measurements on the outside.

The hardness obtained is shown in table 5.

The hardness of the samples was intended to reach 95 HB as a minimum hardness requirement, with the samples supplied with hardness above 100 HB. In order to facilitate the analysis of the results, Table 6 was set up, showing the range of hardness per family.

Through the results presented by bands and by the individual results, it is possible to declare that the parameters used for the heat treatment of solubilization and aging were appropriate, since the samples of the CPAMA I family were successful in reaching the specified hardness. The samples from the CPAMA II family did not reach the specified minimum hardness, suggesting that the tempering temperature was below the solubilization level of the alloy. The samples from the CPAMR family did not reach the specified minimum hardness and the group showed lower hardness than the CPAMA II family, considering that the temperature for quenching was the same used in the CPAMA I family, indicating that possibly the

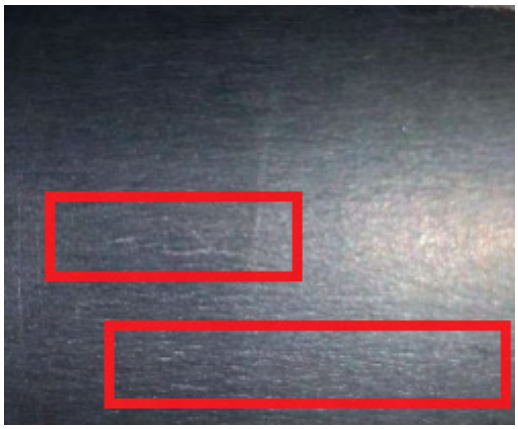

Figure 13 - CPTAMTA Specimen Surface.

Figure 14 - Hot Formed Specimen Surface.

CP	Before aging		After aging	
	X (114,84 mm)	Y (79,62 mm)	X (114,84 mm)	Y (79,62 mm)
CPAMR 1	117,7	81,7	117,6	81,7
CPAMR 2	117,8	81,7	117,8	81,3
CPAMR 3	118,0	82,3	118,0	81,8
CPAMR 4	118,0	81,6	118,2	81,7
CPAMR 5	118,8	81,5	118,7	81,7
CPAMR 6	117,8	81,6	117,9	81,4
CPAMR 7	118,1	81,9	118,1	81,2
CPAMA I 1	118,5	81,8	117,6	82,6
CPAMA I 2	124,0	79,8	124,2	80,2
CPAMA I 3	124,1	81,1	123,8	80,5
CPAMA I 4	123,8	81,4	123,1	80,9
CPAMA I 5	123,0	80,5	123,3	80,9
CPAMA I 6	121,4	81,2	121,8	81,2
CPAMA I 7	123,4	81,1	123,0	80,8

CPAMA II 1	121,9	80,6	121,9	81,3
CPAMA II 2	121,2	81,1	121,2	81,5
CPAMA II 3	122,4	81,0	122,8	81,6
CPAMA II 4	121,9	80,6	122,0	80,8
CPAMA II 5	122,2	80,9	121,2	80,9
CPAMA II 6	122,2	80,9	122,3	80,5
CPAMA II 7	122,0	81,1	122,0	81,6
CPTAMTA 1	+155,0	64,8	-	-
CPTAMTA 2	124,0	81,2	-	-
CPTAMTA 3	124,4	80,3	-	-
CPTAMTA 4	126,0	79,8	-	-
CPTAMTA 5	125,9	79,3	-	-
CPTAMTA 6	+146,0	73,1	-	-
CPTAMTA 7	126,2	79,5	-	-

Table 3 - Dimensional Inspection Results.

CP	**Before aging**		**After Aging**	
	Xm (mm)	**Ym (mm)**	**Xm (mm)**	**Ym (mm)**
CPAMR	118,0±0,3	81,8±0,2	118,0±0,3	81,5±0,2
CPAMA I	122,6±1,9	81,0±0,6	122,4±2,1	81,0±0,7
CPAMA II	122,0±0,4	80,9±0,2	121,9±0,5	81,2±0,4
CPTAMTA	125,3±0,7	80,0±0,7	-	-

Table 4 - Averages with Standard Deviation of Dimensional Inspection.

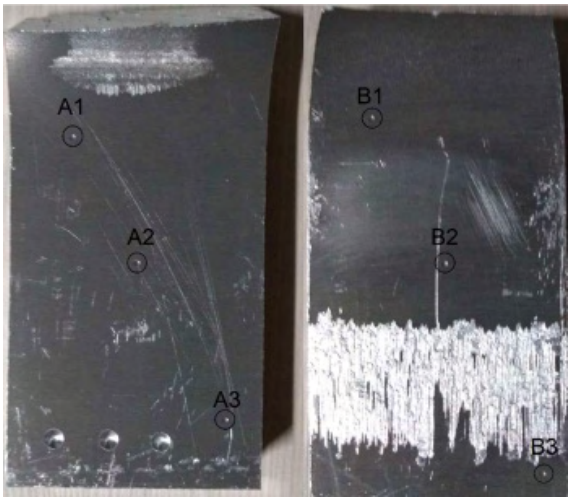

Figure 15 - Hardness Measurement Points/

Group	CP	A1 (HB)	A2 (HB)	A3 (HB)	B1 (HB)	B2 (HB)	B3 (HB)
CPAMR	1	55,5	44,6	41,7	58,1	46,9	42,8
	2	58,1	52,1	43,8	62,1	51,2	46,5
	3	58,7	48,1	42,1	49,4	54,5	47,7
	4	67,1	60,9	58,1	68,5	64,6	59,2
	5	60,9	62,7	55,0	71,3	63,9	62,1
	6	72,8	60,9	63,3	75,9	70,6	59,2
	7	60,4	60,4	54,0	63,9	68,5	45,3
CPAMA I	1	104,9	112,9	108,8	95,5	118,8	114,4
	2	97,7	93,3	92,3	90,2	87,2	89,2
	3	96,6	100,1	93,3	93,3	91,2	78,3
	4	93,3	76,7	88,2	96,6	95,5	90,2
	5	112,9	114,4	111,5	106,2	102,5	102,5
	6	111,5	110,2	106,2	101,2	107,5	114,4
	7	107,5	93,3	111,5	103,7	107,5	103,7
CPAMA II	1	59,8	59,8	63,9	65,2	66,5	59,8
	2	59,2	67,1	72,8	72,8	64,6	72,8
	3	72,0	66,5	69,9	73,5	70,6	73,5
	4	66,5	66,5	69,2	63,9	70,6	57,6
	5	75,1	75,9	111,5	67,1	72,0	71,3
	6	53,5	52,1	59,8	62,7	61,5	60,4
	7	61,5	63,9	62,7	63,9	67,8	65,8
CPTAMTA	1	98,9	89,2	85,3	92,3	94,4	92,3
	2	98,9	86,3	93,3	94,4	92,3	87,2
	3	90,2	93,3	90,2	95,5	91,2	91,2
	4	90,2	88,2	88,2	88,2	85,3	85,3
	5	103,7	84,4	84,4	91,2	81,7	92,3
	6	96,6	90,2	86,3	91,2	86,3	87,2
	7	93,3	93,3	93,3	98,9	95,5	93,3

Table 5 - Hardness Results.

CP	A1 (HB)	A2 (HB)	A3 (HB)	B1 (HB)	B2 (HB)	B3 (HB)
CPAMR	55,5 - 72,8	44,6 - 62,7	41,7 - 63,3	49,4 - 75,9	46,9 - 70,6	42,8 - 62,1
CPAMA I	93,3 - 112,9	76,7 - 114,4	88,2 - 111,5	90,2 - 106,2	87,2 - 118,8	78,3 - 114,4
CPAMA II	53,5 - 75,1	52,1 - 75,9	59,8 - 111,5	62,7 - 73,5	61,5 – 72	57,6 - 73,5
CPTAMTA	90,2 - 103,7	84,4 - 93,3	84,4 - 93,3	88,2 - 98,9	81,7 - 95,5	85,3 - 93,3

Table 6 - Hardness by range.

parameter that influenced these results was the speed of submersion of the specimen in the coolant fluid, in this case, the speed of conformation.

Specifically, the results obtained in the samples of the CPAMR family showed some behaviors that are worth highlighting. For this reason, the graph shown in Figure 16 was prepared, in which the hardnesses of the family were separated according to the measurement region.

It is possible to verify that the measurement regions A1 and B1 (1 and 4 in the graph) showed higher results than the regions A2 and B2 (2 and 5 in the graph) which in turn had higher hardness than the regions A3 and B3 (3 and 6 in the graph), indicating that the initial contact temperature of the specimen with the coolant fluid is an important parameter, along with the speed at which the specimen is immersed in the fluid, as the variation in speed generated hardness ranges in each sample region.

CHARACTERIZATION VIA SEM

A sample of each family was separated for analysis via SEM of the central region of the specimen, the main deformed region. From the results obtained by the analysis, the results through NTS BSD signal will be highlighted, shown in figure 17.

As it can be seen in Figure 17, the samples from the CPAMA I and CPTAMTA families resulted in smaller and more distributed precipitates, thus meeting the hardness requirement, while the samples from the CPAMA II and CPAMR families presented precipitates of heterogeneous sizes and their distribution was not it was uniform. The precipitates are characterized by the white dots in the middle of the matrix shown in Figure 17.

FINAL CONSIDERATIONS

With all the development carried out to apply the concepts of this work, some conclusions were reached regarding each topic.

Regarding the numerical analysis, it was essential, as this feature allowed the work to be more objective in the development of the tool, without the need to manufacture a set of tools and keep making changes in practice, the problems of each tool concept were seen in a different way. preventive, that is, there was no tool try-out, and even so, the matrix used behaved according to the simulation, being resistant enough to support the conformation of the 28 specimens and the thermal cycle of each conformation family.

Regarding the conformation, it can be highlighted the reduction of the pressing force obtained between the hot process compared to the cold process. And also highlighting that while the samples from the hot process were approved in the visual inspection, the samples from the cold process broke or showed a crack, with 100% rejection. Although the proposed process failed in the hardness requirement, it presented the best results in the dimensional analysis, it did not present cracks, showing the possibility of future work varying some parameters for this process, seeking to adapt the hardness to the specifications.

The uniformity of hardness of the tested specimens did not influence the results because the group of samples CPTAMTA presented hardness consistent with the requirements established as minimum for T6 condition. The aging treatment was successful, as the CPAMA I samples, they reached the specified objectives, so the temperature and time parameters used for aging treatment can be excluded, as a possible influence of the test results.

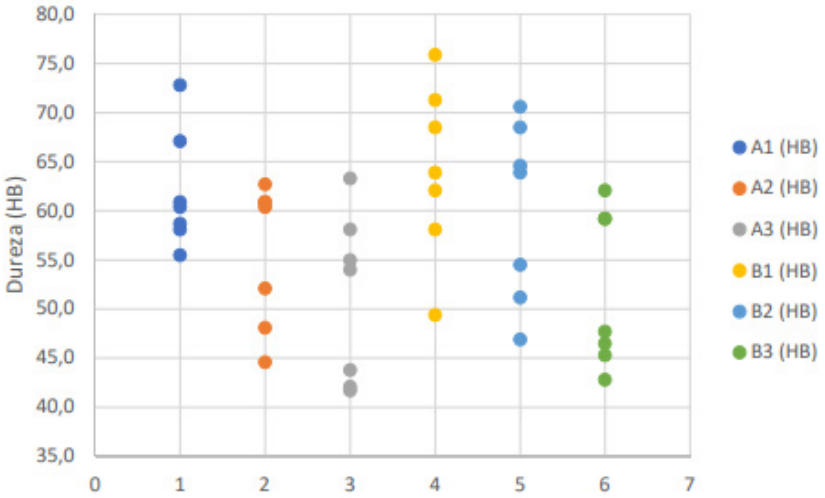

Figure 16 - CPAMR Hardness by Measurement Point.

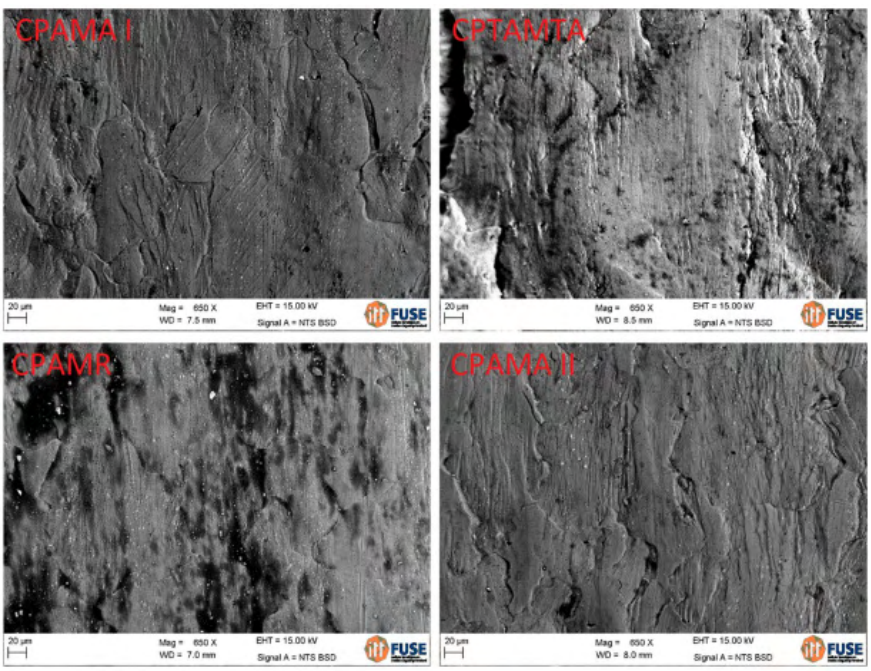

Figure 17 - SEM Samples - NTS BSD.

The results of the CPAMA II samples, although not positive, were better than the CPAMR process, the process proposed in this article, which indicates a strong tendency that the primary factor for the proposed process to be successful is speed. of cooling, in line with this conclusion, hardness values were presented at points A1 and B1, higher than the others, these being the first cooling points. The results of the precipitates presented via SEM, confirm this deduction by showing that the group of samples CPAMA I, which had the heat treatment of solubilization and quenching in a traditional way, had the size of the precipitates smaller and better distributed by the sample, while the CPAMA II group precipitates, which lost heat due to conformation but had a fast quenching, presented larger precipitates, but still well distributed and finally the CPAMR sample precipitates had disproportionate sizes, and were heterogeneously distributed in the sample, being concentrated in some regions and not appearing in others, that is, the time for solubilization was long, allowing the nucleation and growth of precipitates, and these first nucleated precipitates ended up preventing the nucleation of smaller precipitates in the sample matrix.

Another factor to be taken into consideration, in the process is the thickness of the plates, because the smaller, the greater the precipitation rate. In summary, this process can still be analyzed for thin sheets, smaller than 13 mm, or the process can be carried out using mechanical presses, as they have a higher forming speed.

REFERENCES

1. TAN, C.F., SAID, M.R. Effect of Hardness Test on Precipitation Hardening Aluminium Alloy 6061-T6. Chiang Mai J. Sci. Vol 36, Nº3, pp. 276-286, 2009.

2. OZTURK, F., SISMAN, A., TOROS, S., KILIC, S., PICU, R.C., Influence of Aging Treatment on Mechanical Properties of 6061 Aluminum Alloy. Materials and Design. Vol 31, pp. 912-975, 2009.

3. KIM, Y.H., RYOU, T.K., CHOI, H.J., HWANG, B.B. Na Analysis of the Forging Processes for 6061 Aluminum-Alloy Wheels. Journal of Materials Processing Technology. Vol 123, pp270-276, 2002.

4. SOARDI, A., LUCHEZI, C., MARCHETT, J.V.H., Silva, R.C., SCHAEFFER, L. Análise das Deformações em um Processo de Dobramento Variando a Geometria da Ferramenta. 39th Senafor, 2019.

5. DE COSTA, L.L., SCHAEFFER, L. Influência de Elementos Microligantes na Microestrutura e Propriedades Mecânicas de Aços Forjados a Quente. 35th Senafor, 2015

6. NORTON, R.L. Projetos de Máquinas: Uma abordagem integrada. 4.ed. Porto Alegre: Bookman, 2013. p.303-399, 481-518, 987.

7. ABAL. Fundamentos e Aplicações do Alumínio. 2.ed. São Paulo: Associação Brasileira do Alumínio, 2007.

8. ABAL. Guia Técnico do Alumínio: Tratamento Térmico do Alumínio e suas Ligas. 2.ed. São Paulo: Associação Brasileira do Alumínio, 2011.